

# THE HUBBLE CONSTANT FROM SZE MEASUREMENTS IN LOW-REDSHIFT CLUSTERS

BRIAN S. MASON, STEVEN T. MYERS, & A.C.S. READHEAD

*105-24 Caltech*

*Pasadena, CA 91125*

*Email: bsm@astro.caltech.edu*

We present a determination of the Hubble constant from measurements of the Sunyaev-Zeldovich Effect (SZE) in an orientation-unbiased sample of 7  $z < 0.1$  galaxy clusters. With improved X-ray models and a more accurate 32-GHz calibration, we obtain  $H_0 = 64_{-11}^{+14} \pm 14_{sys} \text{ km sec}^{-1} \text{ Mpc}^{-1}$  for a standard CDM cosmology, or  $H_0 = 66_{-11}^{+14} \pm 15_{sys} \text{ km sec}^{-1} \text{ Mpc}^{-1}$  for a flat  $\Lambda$ CDM cosmology. The random uncertainty in this result is dominated by intrinsic CMB anisotropies, and the systematic uncertainty is chiefly due to uncertainties in the X-ray spectral models. The implications of this result and future prospects for the method are discussed.

## 1 Introduction

For over two decades it has been known that the combination of X-ray and SZE observations of rich galaxy clusters, under the assumption of spherical symmetry, yields a direct measurement of the cosmic distance scale<sup>1,2</sup>. This comes about due to the fact that the X-ray brightness of a cluster depends upon a different power of  $h$  than the SZE (which is unaffected by cosmological surface brightness dimming), allowing the radio decrement,  $\Delta T_{obs} \equiv q$ , to be predicted from the X-ray data up to a power of  $h$ :  $\Delta T_{pred} \equiv p h^{-1/2}$ . Then  $h$  is given by

$$h = \left( \frac{p}{q} \right)^2. \quad (1)$$

Only in the past few years have reliable and accurate applications of this method become possible<sup>3,4,5,6,7</sup>. Due to the assumption of spherical symmetry in this analysis, selection biases have been a great concern in using the SZE as a distance measure. To address this concern Myers *et al.* (1997) defined an X-ray flux-limited sample of 11  $z < 0.1$  clusters and began a campaign to measure distances to these clusters. With this strategy, random departures from spherical symmetry in individual clusters will not bias the sample average for  $H_0$ . With observations of 4 clusters Myers *et al.* obtain a Hubble Constant of  $54 \pm 14 \text{ km sec}^{-1} \text{ Mpc}^{-1}$ . The accuracy of this result is limited by a 7% radio calibration uncertainty and estimated 15-30% X-ray model uncertainties for each cluster. In this proceeding, we present more recent observations in the campaign initiated by Myers *et al.*, and discuss other improvements in these results.

Our efforts are concentrated on reducing and understanding the uncertainties in the X-ray models, since these have always been a limiting consideration for the SZE. This is facilitated by the advent of abundant X-ray data from ROSAT and other satellites. In addition, we have conducted an absolute radio calibration program at the Owens Valley Radio Observatory (OVRO) which has reduced our calibration uncertainties by over a factor of two. We have also quantitatively evaluated the

effect of CMB anisotropies on our observations.

Throughout this proceeding we use  $H_0 = 100 h^{-1} \text{km sec}^{-1} \text{Mpc}^{-1}$ . We will consider two cosmologies: SCDM ( $\Omega_m = 1, \Omega_\Lambda = 0$ ), and  $\Lambda$ CDM ( $\Omega_m = 0.3, \Omega_\Lambda = 0.7$ ).

## 2 Cluster Sample

In defining a sample for SZE-based  $H_0$  determinations the most important consideration is that the sample be free of any orientation bias, such as would be introduced, *e.g.*, by a surface brightness selection. This is especially important due to the fact (Eq 1) that systematic errors in the observations enter quadratically into the final  $H_0$  result. Since X-ray cluster catalogs are most reliable at high flux levels— and the optical catalogs which underlie most current X-ray cluster catalogs are most reliable at low redshifts— a low- $z$  sample is indicated. This has the additional advantage that the X-ray models will be better since, at low- $z$ , the signal is stronger and angular resolution is less of an issue.

Mason & Myers (2000) define an expanded, X-ray flux-limited cluster sample of  $z < 0.1$  objects. This is a 90% volume-complete sample selected from the XBAC catalog<sup>10</sup> with the restrictions  $F_X > 1.0 \times 10^{-11} \text{erg cm}^{-2} \text{s}^{-1}$ . At  $z = 0.1$ , the volume-completeness criterion corresponds to  $L_X > 1.13 \times 10^{44} h^{-2} \text{erg s}^{-1}$  (0.1 - 2.4 keV). The resulting set of 31 clusters contains the Myers *et al.* sample. Although the XBAC sample is ultimately derived from an optical catalog, the bright, rich clusters which pass our luminosity criterion should be reliably selected in any orientation. The 7 clusters for which we present measurements here are all members of the smaller Myers *et al.* sample, but this work is part of an ongoing project to survey distances to the objects in our expanded sample.

## 3 X-ray Models

Mason & Myers (2000) also present X-ray models for the 22 of the 31 clusters which had public ROSAT PSPC data as of May 1999. The primary focus of this analysis was to quantify the uncertainty in the beam-convolved inverse Compton optical depth,  $\tau_{sw}$ . To do this, the ROSAT PSPC data were smoothed, and  $10^3$  realizations of each cluster were generated including Poisson noise; each realization was analyzed just as we analyzed the real data. We used a similar strategy to quantify errors induced by inaccurate vignetting correction and background subtraction. We find, overall, that the beam-convolved inverse-Compton optical depths are robustly constrained by the ROSAT data, and unaffected by realistic PSPC systematics. As an example, Figure 1 shows the  $10^3$  model predictions for the beam-convolved optical depths ( $\tau_{sw}$ ) from our analysis of the A2142 data. This is an extreme example since we have excised the central region of the PSPC data, which is contaminated by cooling flow emission, and allowed the fit to be completely unconstrained there. The result is that the core radius  $\theta_o$  is poorly determined; nevertheless the overall optical depth is well constrained since the SZ decrement is mostly determined by the extended lines of sight. The cancellation of the large uncertainties in the individual parameters ( $\beta, \theta_o, n_{eo}$ ) comes about due to strong parameter correlations,

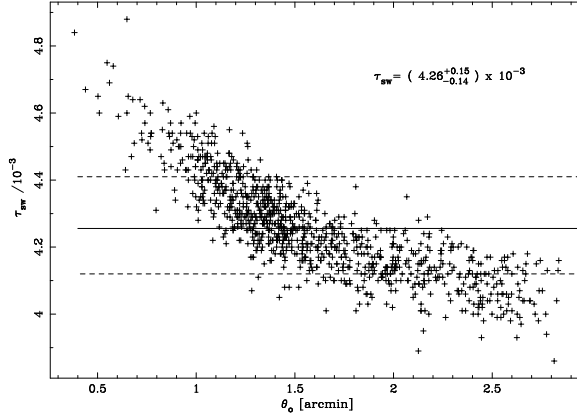


Figure 1. Predictions of the 5.5-meter beam-convolved SZE decrement for A2142. The solid line shows the distribution mean and the dashed lines show two-sided 68% confidence regions.

Table 1. Cluster Model Parameters

Cluster	$z$	$\theta_o$ ( $'$ )	$\beta$	$n_{eo}$ ( $10^{-3} h^{1/2} \text{cm}^{-3}$ )	$kT_e$ (keV)
A399	0.0715	$4.33 \pm 0.45$	$0.742 \pm 0.042$	$3.23 \pm 0.18$	$7.0 \pm 0.2$
A401	0.0748	$2.26 \pm 0.41$	$0.636 \pm 0.047$	$7.90 \pm 0.81$	$8.0 \pm 0.2$
A478	0.0900	$1.00 \pm 0.15$	$0.638 \pm 0.014$	$27.81 \pm 9.7$	$8.4 \pm 0.7$
A1651	0.0825	$2.16 \pm 0.36$	$0.712 \pm 0.036$	$7.14 \pm 3.20$	$6.1 \pm 0.2$
Coma	0.0232	$9.32 \pm 0.10$	$0.670 \pm 0.003$	$4.52 \pm 0.04$	$9.1 \pm 0.4$
A2142	0.0899	$1.60 \pm 0.12$	$0.635 \pm 0.012$	$14.95 \pm 1.0$	$9.7 \pm 0.8$
A2256	0.0601	$5.49 \pm 0.21$	$0.847 \pm 0.024$	$4.08 \pm 0.08$	$6.6 \pm 0.2$

and it is generally important to account for these (*e.g.*, by Monte Carlo methods) in order to understand the uncertainties in the observables.

A summary of the models for the 7 clusters on which we have radio observations is presented in Table 1. For Coma, following Hughes, Gorenstein, & Fabricant (1988), we adopt a hybrid temperature profile which is isothermal inside of  $500 h^{-1} \text{kpc}$  and adiabatic ( $\gamma = 1.5$ ) outside of this. For the other clusters we assume an isothermal profile. We use the global, cooling-flow corrected electron temperatures of Markevitch *et al.* (1998). Our value for  $H_0$  is not sensitive to the temperature profile we assume: it changes by  $< 5\%$  if we assume hybrid profiles for all of the clusters. While more extreme temperature profile models would have a stronger affect on our result, such models are not motivated by current analyses<sup>12,13</sup>.

#### 4 Radio Observations

Table 2. OVRO SZE Observations

Cluster	$y_{obs}$ ( $10^{-5}$ )	significance ( $\sigma$ )
A399	$3.24 \pm 0.41$	2.5
A401	$6.93 \pm 0.46$	5.2
A1651	$4.88 \pm 0.59$	5.6
Coma	$6.38 \pm 1.01$	4.0
A2142	$9.10 \pm 0.52$	6.7
A2256	$5.00 \pm 0.60$	3.6

#### 4.1 Recalibration

In March through May of 1998 we undertook a program of absolute calibration with the OVRO 1.5-meter radio telescope. The gain of this antenna was measured by NIST’s Boulder, CO near-field test range in May of 1990; these measurements in conjunction with accurate total power determinations on-site at OVRO allowed a direct determination of the flux densities of celestial sources. The primary target for this program was the supernova remnant Cassiopeia A (Cas A), the second brightest extrasolar source in the sky at cm wavelengths. We find an epoch 1998 flux density  $S_{CasA,1998} = 194 \pm 4$  Jy at 32.0 GHz. Observations of Jupiter relative to Cas A with the OVRO 5.5-meter telescope give  $T_{Jup} = 152 \pm 5$  K at 32.0 GHz. All of our SZ measurements are referred to this flux density scale, which improves by a factor of two over the uncertainty present in the Myers *et al.* calibration. The absolute calibration measurements are discussed at length in Mason *et al.* (1999), and are the basis of the flux density scales which have been adopted by Saskatoon<sup>16,17</sup>, the 30 GHz channel of MAT<sup>17</sup>, and the CBI<sup>18</sup>; the RING5M<sup>19</sup> calibration is comparable but independent.

#### 4.2 SZE Observations & Effect of the Intrinsic Anisotropy

From October 1996 through March 1998 we observed A399, A401, and A1651 with the OVRO 5.5-meter telescope. The results of these observations, together with measurements of Coma<sup>4</sup> and A2142, A2256, and A478<sup>8</sup>, are shown in Table 2. The errors reported in this table are the observational noise only. The significance of the detection  $\sigma$  is also reported, including the effects of intrinsic CMB anisotropies.

Intrinsic anisotropies on this scale ( $\ell = 590 \pm 200$ ) are known to be significant, although these will be averaged down somewhat by our scan pattern. To evaluate the impact of these anisotropies, we generated  $10^3$  realizations of  $4 \text{ deg}^2$  patches of sky from a  $\Lambda$ CDM power spectrum normalized to the RING5M<sup>19</sup> observed power level. Each realization was convolved with the 5-m main beam and the switching pattern characteristic of a typical SZE observations. We find a residual CMB signal of  $\sigma_{cmb} = 64 \mu\text{K}$ , or  $\sigma_{cmb} = 1.24 \times 10^{-5}$  in terms of the Compton- $y$ , which is accounted for in our  $H_0$  analysis.

## 5 Interpretation & Discussion

When the effects of intrinsic CMB anisotropy are included, faint clusters like A399 are seen to be detected at less than  $3\sigma$ . It is important to keep such clusters in the analysis, however, in order that an orientation bias not be introduced into our result. To account for these low signal-to-noise measurements, we have developed a maximum likelihood method of estimating  $H_0$  from the SZ and X-ray data. Preliminary results from the application of this method to our 7 clusters are shown in Table 3. The calibration uncertainties are 3% (radio) and 8% (X-ray), and we estimate a 10% uncertainty in the SZE predictions due to the possibility of substructure and non-isothermality in the ICM. We find  $H_0 = 64^{+14}_{-11} \pm 14_{sys} \text{ km sec}^{-1} \text{ Mpc}^{-1}$  (SCDM), or  $H_0 = 66^{+14}_{-11} \pm 15_{sys} \text{ km sec}^{-1} \text{ Mpc}^{-1}$  ( $\Lambda$ CDM). Final results on this sample are in press<sup>20</sup>.

The ages implied [ $(10.2 \pm 3.2) \times 10^9$  years SCDM;  $(14.2 \pm 4.5) \times 10^9$  years  $\Lambda$ CDM] are consistent with recent age determinations from main-sequence fitting, which give ages of  $(> 12 \pm 1) \times 10^9$  years<sup>21,22</sup>. From a hydrostatic analysis of 22 X-ray clusters in our sample<sup>9</sup>, together with this value for  $H_0$ , we determine  $\Omega_M = 0.33 \pm 0.05$ . This argues strongly against SCDM cosmologies, and in light of recent CMB measurements<sup>17,19,23</sup> which indicate  $\Omega_{tot} \sim 1$ , may suggest another form of energy density such as the cosmological constant or quintessence<sup>24</sup>. These results are broadly in agreement with the concordance models<sup>25</sup> suggested by a number of independent means.

Coverage of clusters in this sample is continuing with the Cosmic Background Imager<sup>26,27</sup> (CBI). The CBI's greater coverage ( $\sim 20$  clusters) will significantly reduce uncertainties due to intrinsic CMB anisotropies. Although the results we report here incorporate improved X-ray models, the modelling uncertainties will still be the limiting consideration for larger samples. In order to achieve a 10% determination of  $H_0$  from the SZE, a better understanding of the spectral models for the cluster atmospheres will then be essential.

Table 3.  $H_0$  results on 5 Clusters

Cluster	$y_{obs}$ ( $10^{-5}$ )	$y_{pred}$ ( $10^{-5}h^{-1/2}$ )	$H_0$ ( $\text{km sec}^{-1} \text{ Mpc}^{-1}$ )
A399	$3.24 \pm 0.41$	$3.27 \pm 0.20$	$102^{+116}_{-53}$
A401	$6.93 \pm 0.46$	$4.82 \pm 0.32$	$48^{+28}_{-16}$
A478	$7.77 \pm 0.58$	$6.05 \pm 0.54$	$61^{+33}_{-20}$
A1651	$4.88 \pm 0.59$	$2.92 \pm 0.17$	$36^{+35}_{-15}$
Coma	$6.38 \pm 1.01$	$5.00 \pm 0.38$	$62^{+49}_{-24}$
A2142	$9.10 \pm 0.52$	$8.12 \pm 0.74$	$79^{+34}_{-24}$
A2256	$5.00 \pm 0.60$	$4.11 \pm 0.26$	$67^{+62}_{-28}$
SAMPLE	—	—	$64^{+14}_{-11}$

NOTE: Observational and model uncertainties are  $1\sigma$  random errors only.

## Acknowledgments

We are grateful to Russ Keeney for his work on the OVRO 5-meter and 40-meter telescopes, to Jon Sievers for help with the 1997/98 OVRO observations and the CMB simulations, and to Erik Leitch for writing the OVRO data-analysis software. We received support from NSF grants AST 91-19847 and AST 94-19279. STM was supported by an Alfred R. Sloan Fellowship at the University of Pennsylvania.

## References

1. Silk, J. & White, S.D.M., ApJ **226**, L103 (1978)
2. Cavaliere, A., Danese, L., & De Zotti, G., A&A **75**, 322 (1979)
3. Birkinshaw, M., Hughes, J.P., & Arnaud, K.A., ApJ **379**, 466 (1991)
4. Herbig, T., Lawrence, C.R., Readhead, A.C.S., & Gulkis, S., ApJ **449**, L5 (1995)
5. Carlstrom, J., Joy, M., & Grego, L., ApJ **456**, L75 (1996)
6. Grainge, K. *et al.*, MNRAS **278**, L17 (1996)
7. Holzapfel, W.L. *et al.*, ApJ **480**, 449 (1997)
8. Myers, S.T., Baker, J.E., Readhead, A.C.S., Leitch, E.M., & Herbig, T., ApJ **485**, 1 (1997)
9. Mason, B.S. & Myers, S.T., ApJ **540**, 614 (2000)
10. Ebeling, H. *et al.*, MNRAS **281**, 799 (1996)
11. Hughes, J.P., Gorenstein, P., & Fabricant, D., ApJ **329**, 82 (1988)
12. Irwin, J.A., Bregman, J.N., & Evrard, A.E. ApJ **519**, 518 (1999)
13. White, D.A., MNRAS **312**, 663 (2000)
14. Markevitch, M., Forman, W.R., Sarazin, C.L., & Vikhlinin, A., ApJ **503**, 77 (1998)
15. Mason, B.S., Leitch, E.M., Myers, S.T., Cartwright, J.K., & Readhead, A.C.S., AJ **118**, 2908 (1999)
16. Netterfield, C. B.; Devlin, M. J.; Jarolik, N.; Page, L.; Wollack, E. J., ApJ **474**, 47 (1997)
17. Miller, A.D. *et al.*, ApJL **524**, 1 (1999)
18. Padin, S. *et al.*, ApJL *in press* (astro-ph/0012212)
19. Leitch, E.M. *et al.*, ApJ **532**, 37 (2000)
20. Mason, B.S., Myers, S.T., & Readhead, A.C.S., ApJL *in press*.
21. Reid, I.N., AJ **114**, 161 (1997)
22. Chaboyer, B., Demarque, P., Kernan, P.J., & Krauss, L.M., ApJ **494**, 96 (1998)
23. de Bernardis, P. *et al.*, Nature **404**, 955 (2000)
24. Caldwell, R.R., Dave, Rahul, & Steinhardt, Paul J., PRL **80**, 1582 (1998)
25. Bahcall, N., Ostriker, J., & Steinhardt, P.J. Science **284**, 1481 (1999)
26. Udomprasert, P.S., Mason, B.S., & Readhead, A.C.S., to appear in *Constructing the Universe with Clusters of Galaxies*, ed. F. Duret and D. Gerbel, "The Sunyaev-Zel'dovich Effect with the Cosmic Background Imager."
27. Mason, B.S. *et al.*, *this volume*, "Preliminary Results from the Cosmic Background Imager"